15th Australasian Fluid Mechanics Conference
The University of Sydney, Sydney, Australia
13-17 December 2004

Investigation of the Mean Flow Pattern in Zero-Net-Mass-Flux Elliptical-Jets in Cross-Flow using Planar-Laser-Induced Fluorescence

J. Arnaud, S. Tomar and J. Soria

Laboratory for Turbulence Research in Aerospace &
Combustion (LTRAC),
Department of Mechanical Engineering,
Monash University, Melbourne, VIC 3800, Australia

Abstract

Planar-laser-induced fluorescence (PLIF) measurements have been used to investigate the mean flow pattern of a zero-net-mass-flux elliptical jets in cross-flow (ZNMF-EJICF). This particular jet is generated using the working fluid without net transfer of mass across the system boundary during one period of oscillation. The investigation involves the measurement of the mean jet profiles of the elliptical JICF. Two distinct flow regimes are observed namely single trajectory and multiple trajectory jets. Single trajectory jets demonstrate mixing of the bulk of the fluid outside the upstream boundary layer, while multiple trajectory ZNMF-JICF can penetrate more deeply into the ambient cross-flow. Ensemble-averaged PLIF images of two elliptic jets of aspect ratios (AR) of 2 and 3 exhausting normally into a cross flow with velocity ratios (VR) ranging from 2 to 5 have been studied and compared.

Introduction

Jets in cross-flow (JICF) have many important practical and industrial applications, a few of which include combustion, industrial mixing, injection cooling, pollution transport, cooling of turbine blades, missile control system, etc. Over the past few decades, the JICF has attracted a considerable amount of research interest. Substantial research has been done on jets over the years to reveal their trajectory, spreading and mixing as a function of various flow parameters such as Reynolds number, Strouhal number and ratio of jet-flow to cross-flow momentum [1,2,5]. Previous research based on continuous, pulsed or Zero-Net-Mass-Flux jets suggest that a presence of cross flow enhances the mixing of the jet as compared to a free jet [4,14].

A ZNMF jet is a fluid stream with non-zero mean stream wise momentum formed by the interaction of vortices. The vortices are generated by the periodic oscillation of a fluid. Since there is no net mass of fluid added to the system, the jet formation occurs within the working fluid stream. In the present study, the time-averaged flow across the jet orifice is equal to zero, thus forming a zero-net-mass-flow jet in cross-flow (ZNMF-JICF).

While most studies on JICF phenomenon concentrated their efforts on the circular jet geometry, it is believed that jets of other geometries can also be of immense potential, especially in the area of passive mixing. Previous studies have shown that even in the free jet configuration, continuous or pulsed non-circular geometries (i.e., square, rectangular, elliptic and lobed) exhibit higher mixing rates than a circular geometry [6-13]. Therefore the motivation of this study is to investigate qualitatively the flow pattern of ZNMF-EJICF.

Experimental Apparatus And Method

The experimental investigation was carried out in a square 250 mm closed-circuit vertical water tunnel at the Laboratory for Turbulence Research in Aerospace and Combustion (LTRAC) at Monash University, Melbourne, Australia.

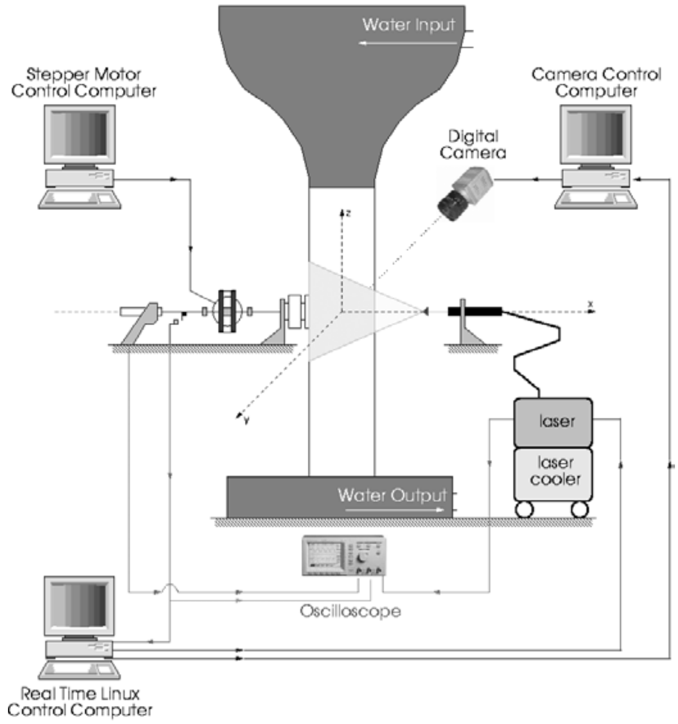

Fig. 2. The experimental setup used for firing the laser and acquiring images using a digital camera.

The tunnel, shown in figure 1, has a 1.5m long working section made of 15mm thick Perspex. Water is introduced into the settling chamber using a spray system at the top, which is then passed through a perforated plate, four stainless steel wire screens, a honeycomb and a 16:1 contraction before entering the working section of the water tunnel.

The creation of the ZNMF jet is produced through an orifice by a piston oscillating in a cylinder. The piston is connected through a scotch-yoke mechanism driven by a stepper motor. The entire set-up is mounted on a horizontal support plate bolted to the tunnel test section wall 550mm below the contraction exit. The arrangement of the apparatus is shown in figure 2.

The scotch-yoke mechanism, which is driven by a stepper motor is controlled by a software program running in Windows operating system. The scotch-yoke mechanism can be driven at amplitudes of 1, 2, 4, 6, 10, 14 and 22mm. It is capable of producing frequencies as low as 0.01Hz. The upper limit of frequencies depends on the choice of the amplitude of motion of the piston and is shown in the table1.

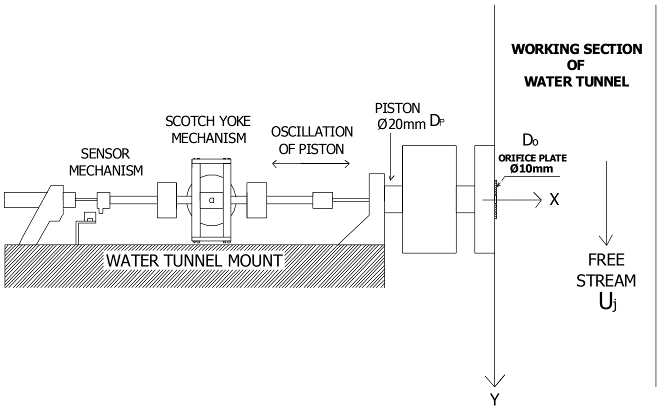

Fig. 2. Arrangement and details of zero-net-mass-flux injection apparatus in the vertical water tunnel [15].

a (mm)	1	2	4	6	10	14	22
f_{max} Hz)	5	6	8	8	6	4	2

Table 1. The upper limit of frequencies depends on the choice of the amplitude of motion of the piston

PLIF Technique

Fluorescent dye flow visualizations were carried out to provide a qualitative picture of these ZNMF-EJICF using a laser sheet generated by a Quanta System 200 mJ dual cavity Nd: YAG laser at a wavelength of 532nm. The sheet was aligned with the orifice center in the z=0 plane.
The entire PLIF image acquisition system was controlled using an in-house developed Real-time Linux (RTAI) computer program. The trigger signal, coming from the sensor mechanism, references the maximum forward position. This signal is sent to the Real-time Linux Computer Program, which synchronizes the images acquisition and the laser firing with a time delay corresponding to the phase of interest.
24 instantaneous flow visualization images of the ZNMF-JICF, at 12 different phases ($N\pi/12$, N integer number, $1 \leq N \leq 12$) and in a region measuring 250 x 180 mm, were recorded using a 12 bit 1.3 Mega Pixel (1280 x 1024) PCO Pixelfly CCD camera. The camera was mounted on a vertical rail and the position was measured using a set of rulers installed in the x, y and z-axes. In addition, 256 images of the dye fluorescence in a region measuring 250 x 180 mm were also acquired at random points in the jet cycle. These were then averaged to reveal the mean flow pattern for each jet.

Flow parameterization

The dimensional parameters governing the flow are the hydraulic diameter of the elliptical orifice D_o = 10 mm, the diaphragm diameter D_p = 20 mm, the frequency of oscillation f, the amplitude of oscillation a, the characteristic jet velocity U_j, and the cross-flow velocity U. These form the non-dimensional groups shown below. These groups are identified as: the Reynolds number (Re), the Strouhal number (St), and the Velocity Ratio (VR), respectively.

$$St = \frac{f\, D_0}{U_j} \quad (1)$$

$$Re = \frac{U_j \; D_0}{\nu} \quad (2)$$

$$R = \frac{U_j}{U} \quad (3)$$

The momentum jet velocity, U_j, through the orifice can be calculated from the root mean square piston velocity V_{prm} using equation (4):

$$U_j = \frac{V_{prms} \;\; D_P}{D_0} \quad (4)$$

Making use of the following relationship between the root mean square and peak velocity for a pure sinusoidal oscillation,

$$V_{prms} = \frac{V_{max}}{\sqrt{2}} \quad (5)$$

$$V_{max} = \omega\, a \quad (6)$$

And after substituting Equations (4), (5) and (6) appropriately into equations (1), (2) and (3), the following equations were obtained,

$$St = \frac{D_0^{\;\;2}}{a\sqrt{2}\,\Pi\, D_p} \quad (7)$$

$$U_j = \frac{\sqrt{2}\,\Pi\, f\, a\, D_p}{D_0} \quad (8)$$

$$Re = \frac{\sqrt{2}\,\Pi\, f\, a\, D_p}{\nu} \quad (9)$$

Equations (7), (8) and (9) indicate that the above parameters depend entirely on the geometrical aspects of the experimental set-up and the frequency of motion of the piston.

Experimental Conditions

To identify the various flow regimes of the ZNMF-EJICF, 40 different jets were formed by varying the tunnel speed U, the oscillation frequency, the amplitude of the diaphragm oscillations and the aspect ratio.

VR	Re	a (mm)	St	f (Hz)	Uj (m/s)	U (m/s)
2	1066	2	0.563	6.00	0.107	0.053
2	1066	4	0.281	3.00	0.107	0.053
2	1066	6	0.188	2.00	0.107	0.053
2	1066	10	0.113	1.20	0.107	0.053
2	1066	14	0.080	0.86	0.107	0.053
3	1066	2	0.563	6.00	0.107	0.053
3	1066	4	0.281	3.00	0.107	0.053
3	1066	6	0.188	2.00	0.107	0.053
3	1066	10	0.113	1.20	0.107	0.053
3	1066	14	0.080	0.86	0.107	0.053
4	1066	2	0.563	6.00	0.107	0.027
4	1066	4	0.281	3.00	0.107	0.027
4	1066	6	0.188	2.00	0.107	0.027
4	1066	10	0.113	1.20	0.107	0.027
4	1066	14	0.080	0.86	0.107	0.027
5	1066	2	0.563	6.00	0.107	0.027
5	1066	4	0.281	3.00	0.107	0.027
5	1066	6	0.188	2.00	0.107	0.027
5	1066	10	0.113	1.20	0.107	0.027
5	1066	14	0.080	0.86	0.107	0.027

Table 2. Jet parameters used for qualitative PLIF experiments.

The generation parameters for elliptical jets of AR = 2 and AR = 3 are summarized in Table 2. Only certain necessary characteristics of the ZNMF-EJICF have been discussed in this study.

Results

Instantaneous Flow Pattern

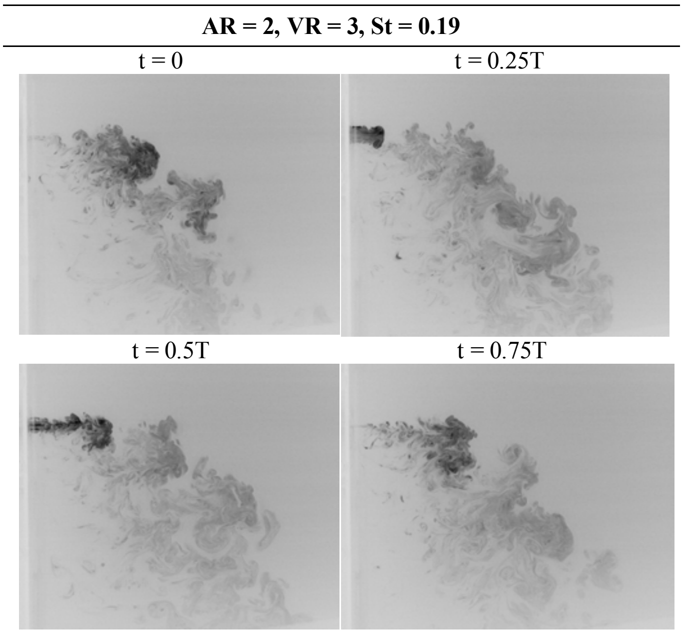

Fig 3. Instantaneous PLIF measurements of a single trajectory.

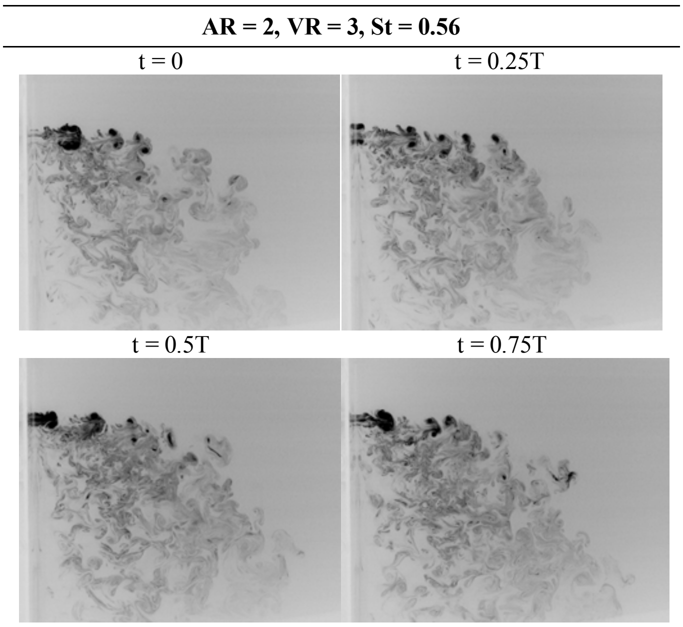

Fig. 4 Instantaneous PLIF measurements of a multiple trajectory.

The instantaneous PLIF measurements of single and multiple trajectory ZNMF elliptical-JICF are shown in figures 3 and 4 respectively. They clearly show the emergence of the jet and formation of a vortex ring pair that is gradually carried into the cross flow. At cycle start time, t = 0, the piston is at its maximum back position in the cylinder and hence, the velocity of the piston is zero at this particular point. The backward stroke of the piston caused the fluid to be "sucked in" from the mainstream into the cylinder. At t = 0.25T, the piston is moving forward in the cylinder and hence "pushing" the fluid out of the orifice plate, which results in the generation of the ZNMF jet. At the next phase, t = 0.5T, the entire fluid in the cylinder has been expelled for the creation of the jet. The piston is at its maximum forward position in the cylinder and is at zero velocity. As a result there is no sucking or pushing occurring. At the last phase, t = 0.75T, the piston is moving back towards the trigger signal [15].

The major differences in the instantaneous patterns of the two jets were the frequency of shedding of the vortex ring pair and the concentration of the dye in the flow frame captured. In the multiple trajectory jets, the dye is convected away by the free-stream fluid a lot slower than the single trajectory jets. This last difference is critical as explained further in the mean flow pattern in the next section.

Main Flow Pattern

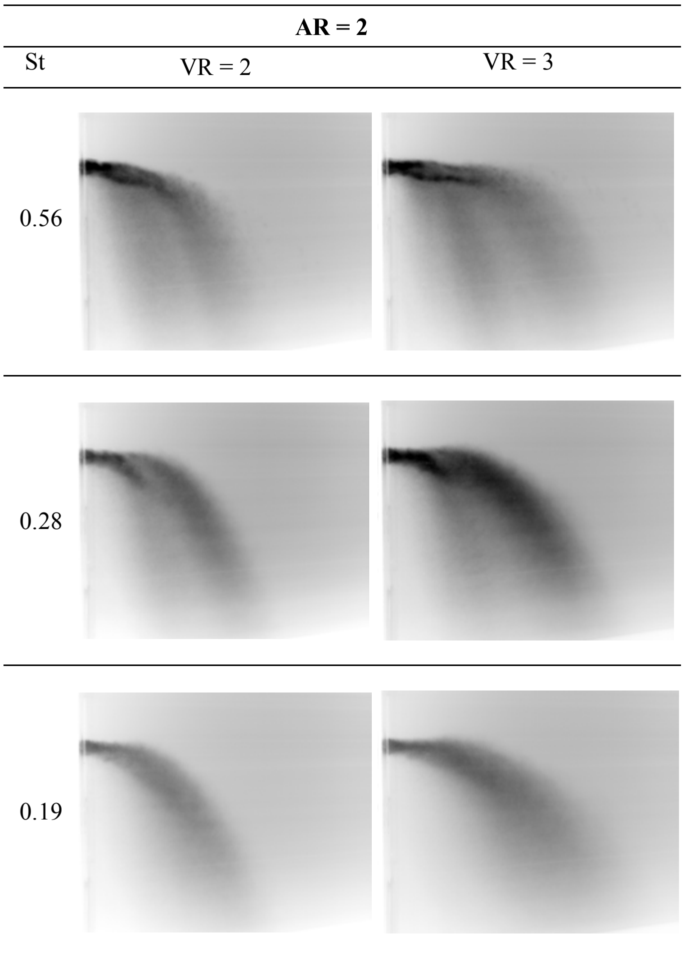

Fig. 5 Main flow pattern for elliptical jets of aspect ratio AR = 2 and velocity ratio VR=2 and VR = 3, and St = 0.56, St = 0.28 and St = 0.19.

The different mean flow patterns are obtained by an ensemble average of 256-single exposed dye flow visualization images and are shown in figures 5 and 6 for the single and multiple trajectory ZNMF-EJICF respectively. The obvious observation made is the dependence between the jet penetration, the elliptical aspect ratio AR and the velocity ratio VR. Penetration of the jet increases with orifices of less aspect ratio as expected. As seen from figures 5 and 6, the mean penetration of the dye also increases with increase in the velocity ratio. A critical Strouhal number was found for the generation apparatus that can be used to distinguish between the two regimes: single trajectory ZNMF-EJICF and multiple trajectory ZNMF-EJICF. By comparing the main flow pattern of figure 5 with those of figure 6, it seems the critical Strouhal number is dependant on the aspect ratio AR. Indeed whereas the critical Strouhal number is for AR = 2: $0.19 < St_{crit} < 0.28$, for AR = 3 the value of the critical Strouhal number increases: $0.28 < St_{crit} < 0.56$. This shows that the critical Strouhal number is dependant on the aspect ratio of the orifice chosen to perform the experiment.

In the two elliptical jets, AR = 2 and AR = 3, the two flow structures: single trajectory and multiple trajectory are only dependent on Strouhal number when $2 \leq VR \leq 5$.

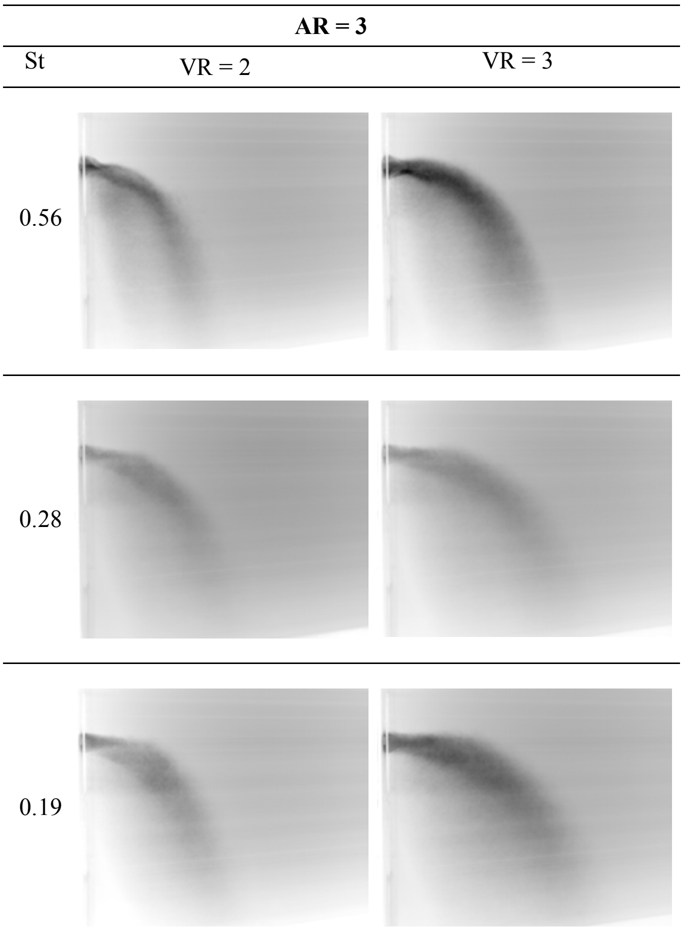

Fig. 6 Main flow pattern for elliptical jets of aspect ratio AR = 3 for velocity ratios of VR=2 and VR = 3, and St = 0.56, St = 0.28 and St = 0.19.

Conclusions

As for circular ZNMF-JICF, single trajectory jets are characterized by a single section of high concentration along the trajectory of the jet whereas multiple trajectory jets are seen to have multiple areas of high concentration. In this case, the multiple trajectory jets are seen to have two distinct areas of maximum concentration, one parallel to the cross flow and the other in the direction of the jet trajectory.

Yet, for elliptical jets the aspect ratio seems to influence the penetration and the value of the critical Strouhal number: the penetration increases with a low aspect ratio and the critical Strouhal number increases with aspect ratio.

Finally, for a fixed aspect ratio and for $2 \leq VR \leq 5$, the two flow structures: single trajectory and multiple trajectory are only dependent on Strouhal number. As decreasing VR increases the distance between the upper and the lower trajectories of multiple trajectory jets, more experiments should be done to investigate the eventual dependence between the critical Strouhal number St_{crit} and the velocity ratio VR.

Acknowledgments

I would like to thank Prof Julio Soria and Mr. Kamal Parker for their help, supervision and patience throughout this project.

References

[1]Cater, J.E. and Soria, J., The evolution of round zero-net-mass-flux-jets, *J. Fluid Mech*., **472**, 2002, 167-200.

[2]Chang, Y.K., and Vakili, A.D., Dynamics of Vortex Rings in Crossflow, *Physics of Fluids*, **7**, 1995, 1583-1597.

[3]Dhanak, M. and de Bernardinis, B., The evolution of an elliptic vortex ring, *J. Fluid Mech.,* **109**, 1981, 189–216.

[4]Eroglu, A., and Breidenthal, R.E., Effects of Periodic Disturbances on Structure and Flame Length of a Jet in a Cross Flow, *AIAA Paper 91-0137*, Jan. 1991.

[5]Gordon, M. and Soria, J., PIV measurements of a zero-net-mass-flux jet in cross flow, *Experiments in Fluids,* **33**, 2002, 863-872.

[6]Grinstein, F., Vortex dynamics and entrainment in rectangular free jets, *J. Fluid Mech*., **437**, 2001, 69–101.

[7]Gutmark, E. and Grinstein, F., Flow control with non-circular jets, *Annu. Rev. Fluid Mech*., **31,** 1999, 239–272.

[8]Ho, C. and Gutmark E., Vortex induction and mass entrainment in a small-aspect-ratio elliptic jet, *J. Fluid Mech.,* **179**, 1987, 383–405.

[9]New, T.H., Lim, T.T. and Luo S.C., A visual study on elliptic jets in cross flow, in: Proceedings of 9th International Symposium of Flow Visualisation, 2000, Paper 224.

[10]New, T.H., T.T. Lim, S.C. Luo, J. Soria, "Particle image velocimetry on elliptic jets in cross flow", in: Proceedings of PIV'01, 2001.

[11]New, T.H. and Soria J., Near-field pairing of leading-edge vortices in elliptic jets in cross flow, *European Journal of Mechanics* B/Fluids, **23**, 2004, 551–569.

[12]Ruggeri, R., Callaghan, E. and Bowden D., Penetration of air jets issuing from circular, square and elliptic orifices directly perpendicularly to an air stream, in: NACA TN 2019, 1950.

[13]Weston, R. and Thames, F., Properties of aspect-ratio 4.0 rectangular jets into a subsonic crossflow, *J. Aircraft* 16, **10**, 1979, 701–707.

[14]Wu, J.M., Vakili, A.D., and Yu, W.K., Mixing of an Acoustically Pulsed Air Jet with a Confined Crossflow, AIAA Journal, **26**, No.8, 1988, 940-947.

[15]Tomar S. and Soria J., MCCDPIV Measurements of a ZNMF JICF, published in the proceedings of PIV'03, Busan, South Korea, 2003